Analytical Biochemistry 468 (2015) 28–33

Contents lists available at ScienceDirect

Analytical Biochemistry

journal homepage: www.elsevier.com/locate/yabio

Validation of endothelin B receptor antibodies reveals two distinct receptor-related bands on Western blot

Travis P. Barr [a], Daniel Kornberg [a], Jean-Pierre Montmayeur [a], Melinda Long [a], Stephen Reichheld [a], Gary R. Strichartz [a,b,*]

[a] Pain Research Center, Department of Anesthesiology, Perioperative and Pain Medicine, Brigham & Women's Hospital, Boston, MA 02115, USA
[b] Department of Biological Chemistry and Molecular Pharmacology, Harvard Medical School, Boston, MA 02115, USA

ARTICLE INFO

Article history:
Received 17 June 2014
Received in revised form 29 August 2014
Accepted 8 September 2014
Available online 16 September 2014

Keywords:
Endothelin B receptor
Antibody
Western
Immunoblot

ABSTRACT

Antibodies are important tools for the study of protein expression but are often used without full validation. In this study, we used Western blots to characterize antibodies targeted to the N or C terminal (NT or CT, respectively) and the second or third intracellular loop (IL2 or IL3, respectively) of the endothelin B receptor (ETB). The IL2-targeted antibody accurately detected endogenous ETB expression in rat brain and cultured rat astrocytes by labeling a 50-kDa band, the expected weight of full-length ETB. However, this antibody failed to detect transfected ETB in HEK293 cultures. In contrast, the NT-targeted antibody accurately detected endogenous ETB in rat astrocyte cultures and transfected ETB in HEK293 cultures by labeling a 37-kDa band but failed to detect endogenous ETB in rat brain. Bands detected by the CT- or IL3-targeted antibody were found to be unrelated to ETB. Our findings show that functional ETB can be detected at 50 or 37 kDa on Western blot, with drastic differences in antibody affinity for these bands. The 37-kDa band likely reflects ETB processing, which appears to be dependent on cell type and/or culture condition.

Endothelin B receptors (ETBs)[1] are extensively studied due to widespread expression and importance in a variety of physiological functions in the cardiovascular, gastrointestinal, excretory, and nervous systems [1–3]. Antibodies are an essential research tool for the localization and quantification of ETB expression through techniques such as immunohistochemistry and Western blot. These techniques rely on the affinity and specificity of the antibodies used; however, many studies employ antibodies that have not been fully validated. Identifying ETB expression using Western blot is further complicated by published reports that ETB can appear at either 50 kDa, the predicted molecular weight for the full-length receptor, or approximately 37 kDa, due to modifications such as N-terminal cleavage [4–8]. There is also currently no knowledge regarding antibody cross-reactivity between these two different molecular weight forms.

In this study, we tested the ability of four commercially available antibodies targeted to different epitopes of ETB to detect endogenous and transfected ETBs using Western blot (Table 1). Primary rat astrocytes and rat brain homogenates were used as sources of endogenously expressed ETB, whereas native and ETB-transfected human embryonic kidney (HEK293) cells were used as negative and positive controls, respectively [9–11].

Materials and methods

Cell culture

Primary rat astrocytes were purchased from Lonza (Basel, Switzerland) and grown in astrocyte growth medium according to the manufacturer's instructions. HEK293 cells, a generous gift from P. Hogan (Harvard Medical School), were grown in Dulbecco's modified Eagle's medium (DMEM, Invitrogen, Carlsbad, CA, USA). Medium for transfected HEK293 cells was supplemented with 500 μg/ml geneticin (Invitrogen). All cells were cultured with 0.5% penicillin/streptomycin (Invitrogen) in a humidified incubator

* Corresponding author at: Pain Research Center, Department of Anesthesiology, Perioperative and Pain Medicine, Brigham & Women's Hospital, Boston, MA 02115, USA. Fax: +1 617 730 2801.
E-mail address: gstrichz@zeus.bwh.harvard.edu (G.R. Strichartz).

[1] *Abbreviations used:* ETB, endothelin B receptor; HEK293 cells, human embryonic kidney cells; ET-1, endothelin-1; BCA, bisinchoninic acid; SDS, sodium dodecyl sulfate; PAGE, polyacrylamide gel electrophoresis; PVDF, polyvinylidenefluoride; TBST, Tris-buffered saline and 0.05% Tween 20; GAPDH, glyceraldehyde-3-phosphate dehydrogenase; ANOVA, analysis of variance; qPCR, quantitative polymerase chain reaction; cDNA, complementary DNA; CycloA, cyclosporin A; fura-2 AM, fura-2 acetoxymethyl ester; mRNA, messenger RNA; ETA, endothelin A receptor; IL2, second intracellular loop; NT, N terminal; CT, C terminal; IL3, third intracellular loop.

http://dx.doi.org/10.1016/j.ab.2014.09.004
0003-2697/

at 37 °C and 5% CO_2. When down-regulation of ETB was required, astrocytes were treated with endothelin-1 (ET-1, 100 nM) and cycloheximide (20 μg/ml) by adding these reagents into their normal culture medium. Samples were collected 24 h after this treatment.

Western blot

Rat brain extract was purchased from Boston Bioproducts (Ashland, MA, USA). Cultured cells were lysed for 10 min in ice-cold RIPA buffer containing 3% protease inhibitor (Sigma–Aldrich, St. Louis, MO, USA) and then centrifuged at 14,000*g* for 20 min at 4 °C. Supernatants were collected and stored at −80 °C with protein concentrations determined using a BCA (bisinchoninic acid) assay kit according to the manufacturer's instructions (Pierce, Tewksbury, MA, USA). Protein samples (15 μg/well in 25% Laemmli buffer, Boston BioProducts) and kaleidoscope molecular weight ladders (Bio-Rad, Hercules, CA, USA) were separated by sodium dodecyl sulfate–polyacrylamide gel electrophoresis (SDS–PAGE) on Mini-PROTEAN TGX Precast Gels with a 4 to 15% gradient (Bio-Rad) for approximately 35 min at 150 V in running buffer (25 mM Tris base, 192 mM glycine, and 1% SDS, pH 8.3). Proteins were transferred to a PVDF (polyvinylidenefluoride) membrane (Millipore, Billerica, MA, USA) in transfer buffer (25 mM Tris base, 192 mM glycine, and 20% methanol, pH 8.3) using a wet blotting method at 400 mA for 90 min. The membrane was blocked with 5% Amersham ECL (enhanced chemiluminescence) Blocking Agent (GE Healthcare, Buckinghamshire, UK) in Tris-buffered saline and 0.05% Tween 20 (TBST; Boston BioProducts) for 1 h and then incubated with primary antibody (see Table 1) in TBST with 1% blocking agent at 4 °C overnight. This was followed by three 10-min washes in TBST, a 1-h room temperature incubation with the appropriate horseradish peroxidase (HRP)-conjugated secondary antibody (Santa Cruz goat anti-rabbit or donkey anti-goat; see Table 1) in 1% blocking agent, and then another three 10-min washes in TBST. For chemiluminescence detection, membranes were exposed to SuperSignal West Dura Extended Duration Substrate (Bio-Rad) and visualized using a Bio-Rad ChemiDoc XRS chemiluminescence detector. After labeling with ETB-targeted antibodies, membranes were stripped for 60 min with Restore PLUS Western blot stripping buffer (Thermo Scientific) at room temperature, rinsed three times for 10 min/rinse, reblocked, and incubated overnight at 4 °C with a glyceraldehyde-3-phosphate dehydrogenase (GAPDH)-targeted antibody (Millipore, 1:20,000). Membranes were processed for GAPDH as described above using goat anti-mouse secondary antibody (Santa Cruz, 1:20,000).

Detection and quantification of Western band intensities was conducted using Quantity One software (Bio-Rad). Bands were normalized to GAPDH by dividing the average intensity of the band by the average intensity of the GAPDH band from the same sample labeled on the same gel. These normalized intensity values were then calculated relative to control and statistically analyzed with Statistica software (StatSoft, Tulsa, OK, USA) using analysis of variance (ANOVA) and Dunnett's post hoc tests to determine which groups were significantly different from their respective controls.

Table 1
ETB receptor antibodies

Source	Epitope	Species	[Primary]	[Secondary]	References
Abcam	IL2	Rabbit	1:500	1:1500	[23–25]
Santa Cruz	NT	Goat	1:500	1:1500	[26–29]
Alomone	IL3	Rabbit	1:500	1:1500	[30–32]
Abcam	CT	Rabbit	1:500	1:1500	

Note. IL2, second intracellular loop; NT, N terminal; IL3, third intracellular loop; CT, C terminal.

qPCR

Quantitative polymerase chain reaction (qPCR) was conducted as described previously [12]. RNA was isolated from three separate passages of 80 to 100% confluent cultures using an RNeasy kit (Qiagen, Valencia, CA, USA), after which 1 μg of total RNA was synthesized to complementary DNA (cDNA) using an iScript kit (Bio-Rad). cDNA was amplified using Evagreen PCR supermix on a MiniOpticon thermocycler (Bio-Rad) using the following protocol: 94 °C for 3 min, 45 cycles of 94 °C for 30 s, 60 °C for 30 s and 72 °C for 1 min, and then a melting curve (65–95 °C in 0.5 °C increments) to confirm primer specificity. Two separate qPCR experiments were each conducted in duplicate on three culture samples for a total of four replicates per data point. Data were analyzed using Bio-Rad CFX Manager with ETB expression normalized to the housekeeping gene cyclosporin A (CycloA), adjusting for primer efficiencies calculated using REST 2009 software (Qiagen) from a serial dilution of each primer. Samples prepared substituting reverse transcriptase with RNase-free water failed to amplify any detectable product. Primer sequences for ETB and CycloA have been described previously [12].

Calcium imaging

Calcium imaging experiments were conducted as described previously [12]. Intracellular calcium was determined by excitation microfluorometry using an inverted IX17 microscope (Olympus America, Center Valley, PA, USA) equipped with a Lambda DG-4+ digital camera (Hamamatsu Photonics, Japan). Coverslips were loaded with fura-2 acetoxymethyl ester (fura-2 AM, 4 μM, Invitrogen) in Ringer's solution (155 mM NaCl, 4.5 mM KCl, 2 mM $CaCl_2$, 1 mM $MgCl_2$, 10 mM D-glucose, and 5 mM Hepes, pH 7.4) for 30 min in the dark at room temperature. Intracellular calcium levels were determined by the ratio of fura-2 fluorescence using the equation $\Delta F/F_0 = (F - F_0)/F_0$, where F is the fluorescence light intensity at each time point and F_0 is the baseline fluorescence intensity averaged over 10 s before the stimulus application. Responding cells were defined as those with more than 10% increase in $\Delta F/F_0$. ET-1 (30 nM) was added alone or in combination with BQ-123 (100 nM) or BQ-788 (100 nM) after respective antagonist pretreatment for 5 min. Data were analyzed by *t* test to determine whether BQ-123 or BQ-788 significantly reduced ET-1 calcium responses.

[^{125}I]ET-1 binding

Equilibrium binding studies were conducted on 90% confluent cells in 12-well plates 24 h after seeding, as described previously [12]. All binding studies were conducted in triplicate and performed at 4 °C to prevent receptor internalization. Cells were incubated for 3 h in 1 ml of 0.1% bovine serum albumin (BSA) in culture medium with varying concentrations of ^{125}I-labeled ET-1 alone (saturation experiments) or in the presence of BQ-123 or BQ-788 (competition experiments). [^{125}I]ET-1 in the supernatant and cell lysate was measured in Ecolite(+) Liquid Scintillation Cocktail (MP Biomedicals, Solon, OH, USA) with a Beckman model LS8500 scintillation counter (Beckman, Palo Alto, CA, USA) for 5 min/sample. Specific binding was defined as the difference between total binding and nonspecific binding, with the latter being determined by coincubation with 500 nM unlabeled ET-1. Protein concentration was measured using a BCA protein assay (Pierce, Rockford, IL, USA). For the competition binding studies (see Fig. 1D in Results and Discussion), data were fit using a one-site nonlinear regression analysis in GraphPad Prism (GraphPad Software, La Jolla, CA, USA).

Stable transfection of HEK293 cells

Expression constructs containing the entire ETB coding sequence together with the neomycin resistance gene (a generous gift from A. Oksche, Mundipharma Research, Germany) were sequenced to verify integrity of the coding sequence. Plasmid DNA was prepared for transfection using an endotoxin-free purification kit (Qiagen). The day before the transfection, DNA vectors were enzymatically linearized and subsequently purified by ethanol precipitation. In addition, HEK293 parental cells were seeded onto 6-well plates to obtain 80% confluence the next day. Cells were then transfected using Lipofectamine 2000 (Invitrogen) according to the manufacturer's instructions. Approximately 16 h post-transfection, the cells were transferred into a 10-cm dish and allowed to settle down overnight. The next day, the medium was exchanged for medium supplemented with 0.5 g/L geneticin (Invitrogen). For the next 7 to 10 days, the medium was replaced every day with fresh medium supplemented with geneticin until all of the cells in the untransfected control had died. At this point, clones were isolated by carefully dispensing trypsin over the isolated colonies and transferring each isolated clone into a single well of a 12-well plate containing medium supplemented with geneticin. Clones were isolated for each construct, amplified, and stored in liquid nitrogen.

Results and discussion

ETB expression in transfected HEK293 cells

Native HEK293 cells were chosen as a negative control because we previously showed that these cells lack ETB expression [12]. Native HEK293 cells show almost no ETB messenger RNA (mRNA), and the low levels of [^{125}I]ET-1 binding seen in these cells are concentration-dependently displaced by the endothelin A receptor (ETA)-selective antagonist BQ-123 with an IC_{50} consistent with ETA binding. Native HEK293 cells also do not respond to ET-1 exposure with an increase in intracellular calcium, likely due to minimal expression of ETAs that is below a threshold for triggering detectable release of intracellular calcium [12,13].

Transfection of functional ETB in HEK293 cells was verified by qPCR, calcium imaging, and radioligand binding (Fig. 1). Transfection raised ETB mRNA expression by nearly 800-fold (from 1 ± 0.29 to 797.76 ± 67.24). Calcium imaging demonstrated that transfected receptors couple to intracellular signaling pathways (Fig. 1A and B), and the robust increases in intracellular calcium were significantly reduced by pretreatment with the ETB-selective antagonist BQ-788 (t test, $P < 0.001$) but not the ETA-selective antagonist BQ-123. HEK–ETB cells also showed a strong increase in [^{125}I]ET-1 binding compared with native HEK293 cells (Fig. 1C). [^{125}I]ET-1 binding was dose-dependently displaced by increasing concentrations of the ETB-selective antagonist BQ-788 with a calculated IC_{50} of 165 ± 24 nM (Fig. 1D). Thus, HEK–ETB cells were successfully transfected with functional ETBs that were not present in native HEK293 cells.

Western blot for ETB

Protein samples from rat astrocytes, rat brain homogenates, native HEK293 cells, and HEK–ETB cells were separated by SDS–PAGE, transferred to a PVDF membrane, and labeled with primary antibodies targeted to different epitopes of the ETB (Table 1 and Fig. 2). Primary antibodies were used at 1:500 because prominent bands could be seen for all antibodies at this dilution (Fig. 2). The second intracellular loop (IL2)-targeted antibody labeled a band close to 50 kDa, the expected molecular weight of full-length ETB protein. This band was present in brain, astrocyte, and HEK–ETB samples but not in the native HEK293 samples that lack ETB message or receptor expression (Fig. 2A). Some much less intense bands could also be seen at molecular weights above 50 kDa in brain and astrocyte samples. The N-terminal (NT)-targeted antibody intensely labeled a band at approximately 37 kDa (Fig. 2B). This band was present in astrocyte and HEK–ETB samples but was absent in native HEK293 and brain samples.

The C-terminal (CT)- and third intracellular loop (IL3)-targeted antibodies both intensely immunolabeled bands at approximately 60 kDa in brain, astrocyte, and HEK–ETB samples but were absent in native HEK293 samples (Fig. 2C and D). Bands near 50 kDa could be detected only in some of the ETB-expressing samples, and these bands were far less intense compared with the band seen near 60 kDa. A band near 85 kDa was also seen for both of these antibodies in native HEK293 samples. Numerous other immunoreactive bands could be seen at molecular weights above 50 kDa for both of these antibodies.

To determine whether bands identified by ETB-targeted antibodies represented some form of ETB, samples were taken from astrocytes, known to express ETBs, that were cultured with ET-1 (100 nM) and cycloheximide (20 μg/ml) for 24 h to down-regulate ETBs (Fig. 3). On activation by ET-1, ETBs are internalized and targeted for degradation [14,15]. Concurrent treatment with the protein synthesis inhibitor cycloheximide prevents synthesis of new ETBs to replace those that were degraded. This treatment has previously been shown to reduce ETB expression, as analyzed by Western blot [15].

Intensity of the 50-kDa band labeled by the IL2-targeted antibody was significantly reduced by treatment with ET-1/cycloheximide (Dunnett's test, $P < 0.05$), as was the 37-kDa band labeled by the NT-targeted antibody (Dunnett's test, $P < 0.05$; see Fig. 3B). Importantly, both of these bands were significantly less intense for the ET-1 + cycloheximide cotreatment compared with cycloheximide alone (t test, $P < 0.05$), indicating that these bands represented ETBs. Cycloheximide alone caused an insignificant reduction in the intensity of both these bands (Ps = 0.63 for 50 kDa and 0.15 for 37 kDa). ET-1 treatment alone also had no significant effect (Ps = 0.15 for 50 kDa and 0.88 for 37 kDa), likely due to replacement of internalized and degraded ETB with newly synthesized receptors. ETBs have a proposed role in ET-1 clearance, so rapid replacement of these receptors may aid in this function [16].

The significant reduction in intensities of the 50-kDa band detected by the IL2-targeted antibody and the 37-kDa band detected by the NT-targeted antibody following ET-1 + cycloheximide treatment is strong evidence that these bands indeed represent ETB, although possibly different forms of the receptor. Interestingly, the tested antibodies had strikingly different affinities for these two forms of ETB. The IL2-targeted antibody strongly labeled the 50-kDa form but was unable to detect the 37-kDa form. Conversely, the NT-targeted antibody strongly labeled the 37-kDa form but did not detect the 50-kDa form. Thus, the ability of a primary antibody to detect ETB will be dependent on the form of ETB expressed by the sample, and a combination of antibodies that recognize both forms may be required to accurately confirm or refute ETB expression. A similar problem may arise in immunocytochemical labeling of receptors for which the combined results from several different antibodies may be necessary to validate the presence of endothelin receptors.

The 60-kDa bands recognized by the IL3- and CT-targeted antibodies, in contrast, do not appear to represent any form of ETB. No difference in intensity was seen in response to ET-1/cycloheximide for the 60-kDa band labeled by the IL3-targeted antibody (ANOVA, $P = 0.241$). The intensity of the 60-kDa band labeled by the CT-targeted antibody was actually significantly increased with ET-1/cycloheximide treatment (Dunnett's test, $P = 0.048$) compared with

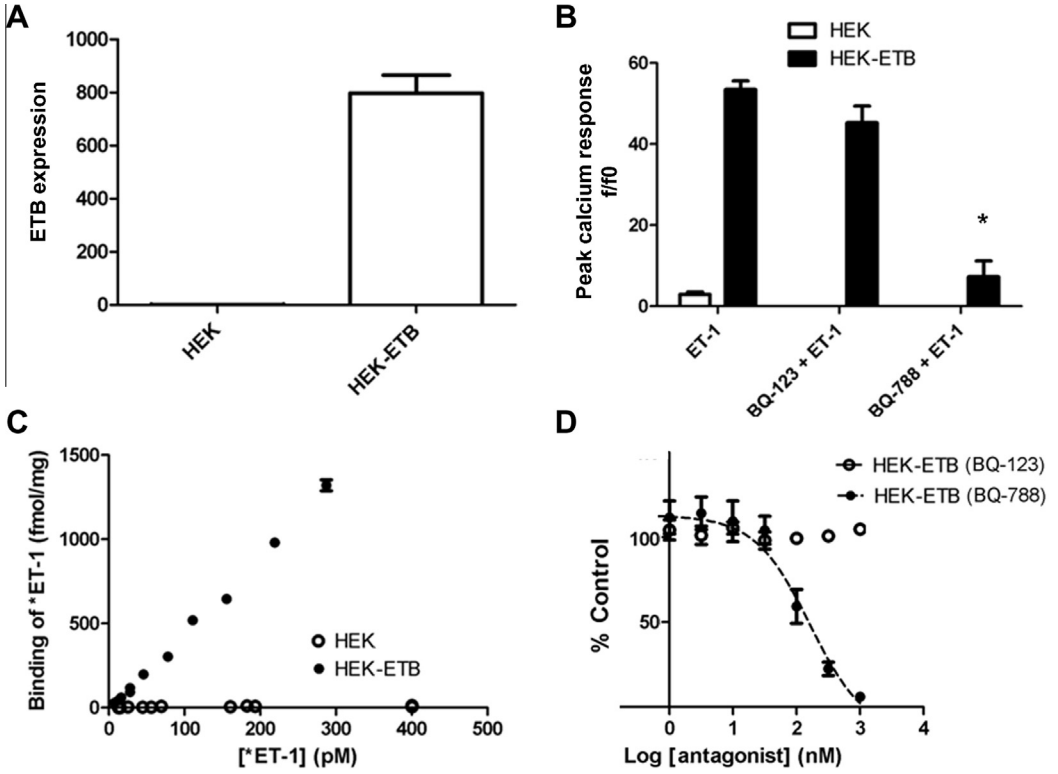

Fig.1. Transfection of functional ETBs in HEK293 cells. (A) qPCR for ETBs in native HEK293 cells (HEK) and HEK293 cells transfected with ETBs (HEK–ETB). ETB mRNA was barely detectable in HEK and was strongly increased, nearly 800-fold, in transfected cells. Data are averages ± standard errors for $n = 3$ with expression normalized to CycloA and shown relative to HEK. (B) Calcium imaging in HEK and HEK–ETB. HEK failed to show an increase in intracellular calcium in response to ET-1 (30 nM). In contrast, HEK–ETB showed a robust increase in intracellular calcium that was significantly reduced by the ETB-selective antagonist BQ-788 (100 nM) but not the ETA-selective antagonist BQ-123 (100 nM). Antagonists were added 5 min before and then together with ET-1 (30 nM). Data are averages ± standard errors for $n = 6$. (C) Saturation binding of [^{125}I] ET-1 in HEK and HEK–ETB. Transfection of ETBs dramatically increased binding of [^{125}I] ET-1 with no signs of saturation at 300 pM [^{125}I] ET-1. (D) Competition binding of BQ-788 with [^{125}I] ET-1 in transfected cells. In HEK–ETB, BQ-788 competed with ET-1 binding in a monotonic fashion with an IC_{50} of 188.6 nM.

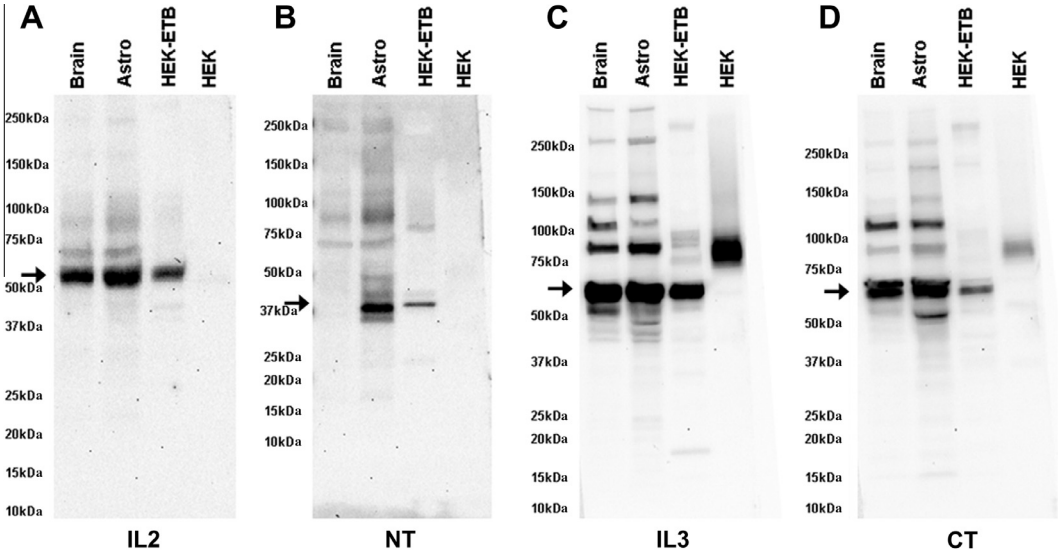

Fig. 2. Primary antibodies were tested for their ability to detect endogenous ETBs in cultured rat astrocytes and rat brain homogenates as well as transfected ETBs in HEK293 cells (HEK–ETB). Arrows show bands of interest that may represent ETBs. (A) The IL2-targeted antibody labeled a prominent band near 50 kDa that was present in rat brain homogenates, astrocytes, and HEK–ETB but not in HEK. (B) The NT-targeted antibody labeled a band near 37 kDa in astrocytes and HEK–ETB but not in HEK or rat brain homogenates. (C and D) IL3- and CT-targeted antibodies both showed a prominent band near 60 kDa in rat brain homogenates, astrocytes, and HEK–ETB that was not present in HEK. A band could be detected near 50 kDa in some ETB-expressing samples, but these bands were far less intense compared with the band near 60 kDa. These antibodies also labeled many other presumably nonspecific bands that varied between samples, including a band near 85 kDa in HEK. Astro, astrocytes.

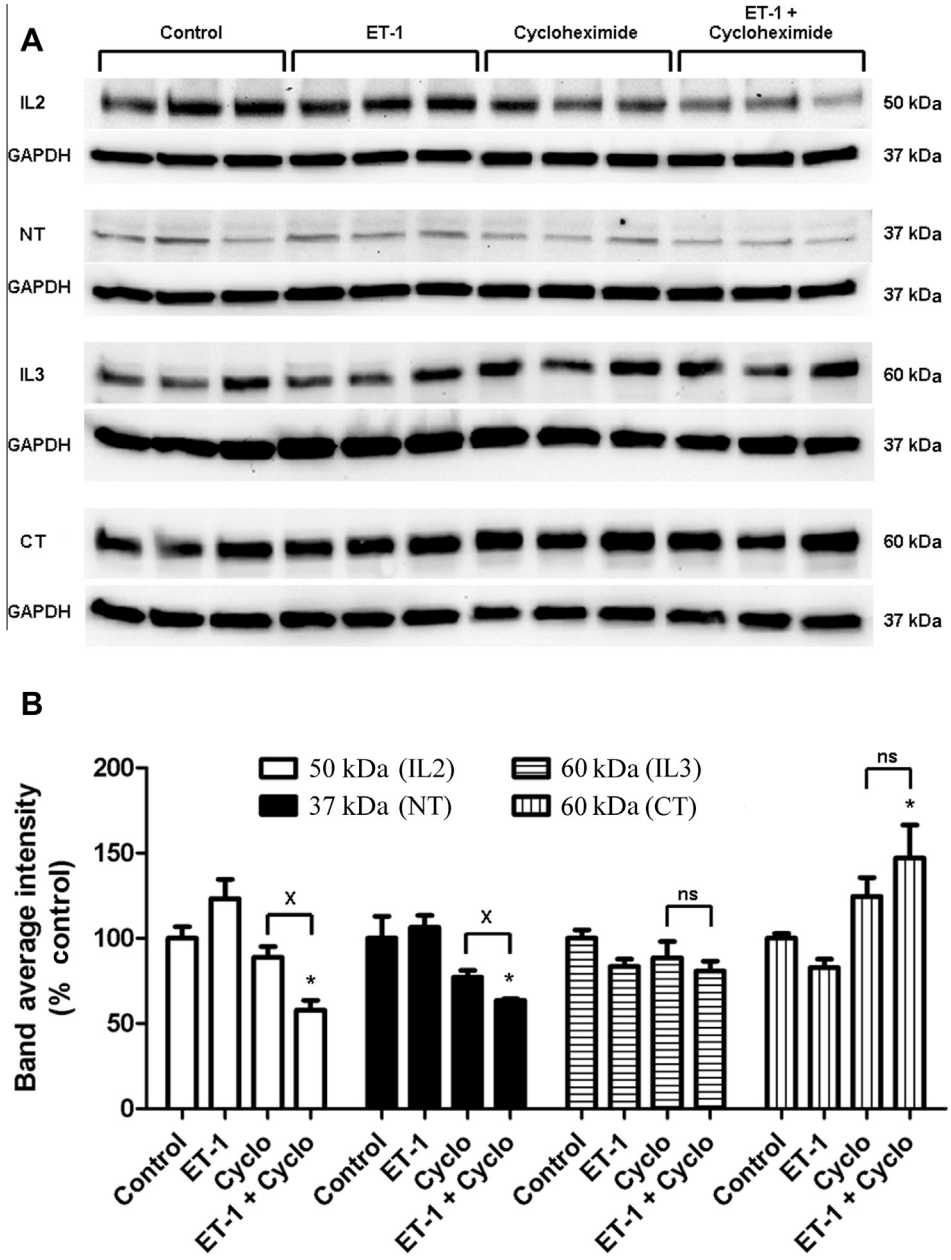

Fig. 3. (A) Representative Western blots from astrocyte samples treated with ET-1 (100 nM) and cycloheximide (20 μg/ml) alone or in combination for 24 h. Bands shown are the 50-, 37-, and 60-kDa bands labeled by the antibody listed in the left column along with corresponding GAPDH bands. As highlighted in Fig. 2, these bands are the most likely to represent ETBs. (B) Quantification of band intensity. Data are shown relative to control after normalization to GAPDH. The 50- and 37-kDa bands labeled by the IL2- and NT-targeted antibodies were significantly less intense in samples from cultures treated with ET-1/cycloheximide. In addition, treatment with ET-1 in the presence of cycloheximide caused a significant reduction in band intensity compared with cycloheximide alone. In contrast, the 60-kDa band labeled by the IL3-targeted antibody showed no difference in intensity across treatment groups, and the 60-kDa band labeled by the CT-targeted antibody was increased by ET-1/cycloheximide treatment. Cyclo, cycloheximide. Bars are averages ± standard errors for $n = 3$. *Dunnett's test, $P < 0.05$, compared with control; ^{X}t test, $P < 0.05$; ns, t test not significant.

control, and there was no significant difference between ET-1 treatment alone and ET-1/cycloheximide used in combination (t test, $P = 0.368$). The lack of a significant reduction in band intensity in response to ET-1/cycloheximide treatment indicates that these 60-kDa bands are not specific to ETB.

Endothelin receptors are known to form homo- and heterodimers [17–21], and endothelin receptor dimerization has been shown to delay internalization, potentially limiting degradation by ET-1 + cycloheximide. However, it seems unlikely that this 60-kDa band represents endothelin receptor homo- or heterodimers given that this molecular weight is less than the expected weights of dimers made from the 37- or 50-kDa monomers.

The 37-kDa band detected by the NT-targeted antibody in astrocyte and HEK–ETB samples is below the molecular weight predicted for the full-length ETB. However, such a 37-kDa band has previously been reported in HEK293 cells transfected with ETBs [5,7,15]. It is unclear what type of receptor processing resulted in the 37-kDa band seen in astrocyte and HEK–ETB samples, but N-terminal cleavage has been shown to result in an approximately 37-kDa band on Western blot in ETB-transfected HEK293 cells as well as vascular smooth muscle and Madin–Darby canine kidney cells [4–7]. The antibody that best labeled this band (NT) in our study was targeted to the N terminus, but the proprietary nature of this antibody's exact epitope makes it uncertain whether this

site would be removed by N-terminal cleavage or whether, in contrast, it could be made more accessible by cleavage of the most proximal portion of the N terminus. This 37-kDa band does not appear to simply be a breakdown product of ETB degradation given that intensity of this band was not increased in astrocytes treated with ET-1 and cycloheximide to down-regulate ETBs (Fig. 3). It is unclear why the 37-kDa band is absent from astrocyte-rich rat brain samples, but it could be due to a difference in receptor processing between cells *in vivo* and those in culture. The 37-kDa band may be a functional ETB given that ETBs have been shown to maintain the ability to bind ET-1 despite N-terminal cleavage [22].

Our results show that some commonly used ETB antibodies do not reliably detect ETB expression by Western blot and that ETBs can appear as either 37- or 50-kDa bands. More research is needed to further characterize ETB processing, but this study suggests that a 37-kDa band can indicate the presence of functional ETBs. Detection of ETBs by Western blot is further complicated by differences in affinity for ETB-targeted antibodies for the 50- and 37-kDa bands; thus, the use of more than one antibody may be necessary to confirm ETB expression depending on the form of ETB present and the primary antibody used.

Acknowledgment

This work was funded in part by U.S. Public Health Service grant R-01 CA080153 to G.R.S.

References

[1] T.P. Barr, S. Kam, A. Khodorova, J.P. Montmayeur, G.R. Strichartz, New perspectives on the endothelin axis in pain, Pharmacol. Res. 63 (2011) 532–540.
[2] A. Khodorova, J.P. Montmayeur, G. Strichartz, Endothelin receptors and pain, J. Pain 10 (2009) 4–28.
[3] G.M. Rubanyi, M.A. Polokoff, Endothelins: molecular biology, biochemistry, pharmacology, physiology, and pathophysiology, Pharmacol. Rev. 46 (1994) 325–415.
[4] N. Foster, T.H. Loi, R. Owe-Young, K.K. Stanley, Lysosomal traffic of liganded endothelin B receptor, Biochim. Biophys. Acta 1642 (2003) 45–52.
[5] E. Grantcharova, J. Furkert, H.P. Reusch, H.W. Krell, G. Papsdorf, M. Beyermann, R. Schulein, W. Rosenthal, A. Oksche, The extracellular N terminus of the endothelin B (ETB) receptor is cleaved by a metalloprotease in an agonist-dependent process, J. Biol. Chem. 277 (2002) 43933–43941.
[6] E. Grantcharova, H.P. Reusch, S. Grossmann, J. Eichhorst, H.W. Krell, M. Beyermann, W. Rosenthal, A. Oksche, N-terminal proteolysis of the endothelin B receptor abolishes its ability to induce EGF receptor transactivation and contractile protein expression in vascular smooth muscle cells, Arterioscler. Thromb. Vasc. Biol. 26 (2006) 1288–1296.
[7] B. Gregan, J. Jurgensen, G. Papsdorf, J. Furkert, M. Schaefer, M. Beyermann, W. Rosenthal, A. Oksche, Ligand-dependent differences in the internalization of endothelin A and endothelin B receptor heterodimers, J. Biol. Chem. 279 (2004) 27679–27687.
[8] A.D. McKelvy, S.M. Sweitzer, Endothelin-1 exposure on postnatal day 7 alters expression of the endothelin B receptor and behavioral sensitivity to endothelin-1 on postnatal day 11, Neurosci. Lett. 451 (2009) 89–93.
[9] H. Ehrenreich, J. Oldenburg, M. Hasselblatt, J. Herms, C. Dembowski, B.M. Loffler, W. Bruck, H. Kamrowski-Kruck, S. Gall, A.L. Siren, L. Schilling, Endothelin B receptor-deficient rats as a subtraction model to study the cerebral endothelin system, Neuroscience 91 (1999) 1067–1075.
[10] F. Lazarini, A.D. Strosberg, P.O. Couraud, S.M. Cazaubon, Coupling of ETB endothelin receptor to mitogen-activated protein kinase stimulation and DNA synthesis in primary cultures of rat astrocytes, J. Neurochem. 66 (1996) 459–465.
[11] J.M. Servitja, R. Masgrau, E. Sarri, F. Picatoste, Involvement of ET_A and ET_B receptors in the activation of phospholipase D by endothelins in cultured rat cortical astrocytes, Br. J. Pharmacol. 124 (1998) 1728–1734.
[12] J.P. Montmayeur, T.P. Barr, S.A. Kam, S.J. Packer, G.R. Strichartz, ET-1 induced elevation of intracellular calcium in clonal neuronal and embryonic kidney cells involves endogenous endothelin-A receptors linked to phospholipase C through Gαq/11, Pharmacol. Res. 64 (2011) 258–267.
[13] Q.L. Zhou, G. Strichartz, G. Davar, Endothelin-1 activates ET_A receptors to increase intracellular calcium in model sensory neurons, NeuroReport 12 (2001) 3853–3857.
[14] T. Bremnes, J.D. Paasche, A. Mehlum, C. Sandberg, B. Bremnes, H. Attramadal, Regulation and intracellular trafficking pathways of the endothelin receptors, J. Biol. Chem. 275 (2000) 17596–17604.
[15] A. Oksche, G. Boese, A. Horstmeyer, J. Furkert, M. Beyermann, M. Bienert, W. Rosenthal, Late endosomal/lysosomal targeting and lack of recycling of the ligand-occupied endothelin B receptor, Mol. Pharmacol. 57 (2000) 1104–1113.
[16] F. Brunner, A.M. Doherty, Role of ET_B receptors in local clearance of endothelin-1 in rat heart: Studies with the antagonists PD 155080 and BQ-788, FEBS Lett. 396 (1996) 238–242.
[17] N.J. Evans, J.W. Walker, Sustained Ca^{2+} signaling and delayed internalization associated with endothelin receptor heterodimers linked through a PDZ finger, Can. J. Physiol. Pharmacol. 86 (2008) 526–535.
[18] R.M. Rapoport, M. Zuccarello, $Endothelin_A$–$endothelin_B$ receptor cross-talk and endothelin receptor binding, J. Pharm. Pharmacol. 63 (2011) 1373–1377.
[19] R.M. Rapoport, M. Zuccarello, $Endothelin_A$–$endothelin_B$ receptor cross talk in endothelin-1-induced contraction of smooth muscle, J. Cardiovasc. Pharmacol. 60 (2012) 483–494.
[20] A. Yatawara, J.L. Wilson, L. Taylor, P. Polgar, D.F. Mierke, C-terminus of ETA/ETB receptors regulate endothelin-1 signal transmission, J. Pept. Sci. 19 (2013) 257–262.
[21] S. Yoon, M. Zuccarello, R.M. Rapoport, $Endothelin_A$–$endothelin_B$ receptor cross-talk in rat basilar artery in situ, Naunyn. Schmiedebergs Arch. Pharmacol. 385 (2012) 437–441.
[22] Y. Saito, T. Mizuno, M. Itakura, Y. Suzuki, T. Ito, H. Hagiwara, S. Hirose, Primary structure of bovine endothelin ETB receptor and identification of signal peptidase and metal proteinase cleavage sites, J. Biol. Chem. 266 (1991) 23433–23437.
[23] S.F. Janssen, T.G. Gorgels, K. Bossers, J.B. Ten Brink, A.H. Essing, M. Nagtegaal, P.J. van der Spek, N.M. Jansonius, A.A. Bergen, Gene expression and functional annotation of the human ciliary body epithelia, PLoS One 7 (2012) e44973.
[24] S.J. Kim, J.S. Kim, S.W. Kim, E. Brantley, S.J. Yun, J. He, M. Maya, F. Zhang, Q. Wu, F. Lehembre, U. Regenass, I.J. Fidler, Macitentan (ACT-064992), a tissue-targeting endothelin receptor antagonist, enhances therapeutic efficacy of paclitaxel by modulating survival pathways in orthotopic models of metastatic human ovarian cancer, Neoplasia 13 (2011) 167–179.
[25] J.S. Speed, B. LaMarca, H. Berry, K. Cockrell, E.M. George, J.P. Granger, Renal medullary endothelin-1 is decreased in Dahl salt-sensitive rats, Am. J. Physiol. Regul. Integr. Comp. Physiol. 301 (2011) R519–R523.
[26] S.C. Chen, C.Y. Lin, Y.H. Chen, H.Y. Fang, C.Y. Cheng, C.W. Chang, R.A. Chen, H.L. Tai, C.H. Lee, M.C. Chou, T.S. Lin, L.S. Hsu, Aberrant promoter methylation of EDNRB in lung cancer in Taiwan, Oncol. Rep. 15 (2006) 167–172.
[27] P. Henno, C. Maurey, C. Danel, P. Bonnette, R. Souilamas, M. Stern, C. Delclaux, M. Levy, D. Israel-Biet, Pulmonary vascular dysfunction in end-stage cystic fibrosis: role of NF-κB and endothelin-1, Eur. Respir. J. 34 (2009) 1329–1337.
[28] W. Tang, B. Li, J. Tang, K. Liu, J. Qin, W. Wu, Q. Geng, J. Zhang, H. Chen, X. Xu, Y. Xia, Methylation analysis of EDNRB in human colon tissues of Hirschsprung's disease, Pediatr. Surg. Int. 29 (2013) 683–688.
[29] M. van den Heuvel, O. Sorop, S.J. Koopmans, R. Dekker, R. de Vries, H.M. van Beusekom, E.C. Eringa, D.J. Duncker, A.H. Danser, W.J. van der Giessen, Coronary microvascular dysfunction in a porcine model of early atherosclerosis and diabetes, Am. J. Physiol. Heart Circ. Physiol. 302 (2012) H85–H94.
[30] A.N. Bramall, M.J. Szego, L.R. Pacione, I. Chang, E. Diez, P. D'Orleans-Juste, D.J. Stewart, W.W. Hauswirth, M. Yanagisawa, R.R. McInnes, Endothelin-2-mediated protection of mutant photoreceptors in inherited photoreceptor degeneration, PLoS One 8 (2013) e58023.
[31] D. Jacques, M. Descorbeth, D. Abdel-Samad, C. Provost, C. Perreault, F. Jules, The distribution and density of ET-1 and its receptors are different in human right and left ventricular endocardial endothelial cells, Peptides 26 (2005) 1427–1435.
[32] A. Rattner, J. Nathans, The genomic response to retinal disease and injury: evidence for endothelin signaling from photoreceptors to glia, J. Neurosci. 25 (2005) 4540–4549.